J. Nano.- Electron. Phys.
1 (2009) No1, P. 52-61

PACS numbers: 43.20.Mv; 43.30. − k; 43.30. + m

FEATURES OF FREQUENCY CHARACTERISTICS OF NORMAL WAVES IN HYDROACOUSTIC WAVEGUIDE

O.R. Lastovenko, V.A. Lisyutin, A.A. Yaroshenko

Sevastopol National Technical University,
33, Universitetskaya Str., 99053, Sevastopol', Ukraine
E-mail: yaroshenko@optima.com.ua

We consider the isovelocity hydroacoustic waveguide with a bottom composed of a liquid intermediate layer and a half-space. Damping in a layer and a half-space is taken into account. Critical modes frequencies subject to the layer depth are determined. Frequency characteristics of the wave numbers, the modulus and the phase of reflection coefficient, the bottom input impedance, the modal absorption coefficients, the phase and the group velocities of normal waves are calculated as well.

Keywords: *NORMAL WAVES, HYDROACOUSTIC WAVEGUIDE, DISSIPATIVE MODE, TRAPPED MODE, REFLECTION COEFFICIENT, INPUT IMPEDANCE, CRITICAL FREQUENCY, ABSORPTION INDEX.*

(Received 14 February 2009, in final form 24 July 2009)

1. INTRODUCTION

One can consider a sea as the shallow one, in which the sound field is determined by the acoustic characteristics of layered bottom and the sound speed profile [1-3]. Then the "very shallow" is the sea, where the influence of the sound speed profile is negligible, but it is necessary to take into account the acoustic energy absorption in a bottom. Considering damping in mediums, the Snell law becomes non-applicable and the critical modes frequencies should be defined in a different way, proceeding from the radiation conditions [4-6]. In this case the eigenmodes for a waveguide with absorbing bottom are divided into the dissipative modes and the trapped ones. The complex wave numbers, corresponding to the eigenmodes, are the solutions of dispersion equation and the radiation condition holds for them, but for dissipative modes the glancing angle of equivalent ray is found to be more than the critical one [6].

For explanation the experimentally detected effects under acoustic waves propagation in a shallow sea the models of horizontally-layered waveguides of different complexity degree with liquid or elastic bottom [1-3, 7-10] were used. For the purpose of conformity improvement the great attention was paid to the consideration both of the sound speed profile and the bottom layering [11, 12].

Taking into account damping in mediums, the layers, located higher than the layer, in which a wave is under the maximal attenuation, should have the determining influence on the acoustic field. The bottom model in the form of the intermediate layer and the half-space corresponds to sludge on a sand-shell substrate. The sound speed in a slimy layer can be a bit more or less than the sound speed in water, and its depth is comparable with the depth of water layer. Such an intermediate layer will have a complex effect on the acoustic waves propagation in a waveguide [13].

2. STATEMENT OF THE PROBLEM

The waveguide model consists of the isovelocity water layer "1" with the depth h, the intermediate bottom layer "2" with the depth d, and the liquid half-space "3". c_1, c_2, c_3 and ρ_1, ρ_2, ρ_3 are the sound speeds in the mediums "1", "2", "3" and their densities, respectively, and $c_1 \le c_2 < c_3$ or $c_2 \le c_1 < c_3$ and $\rho_1 < \rho_2 < \rho_3$. Damping in the mediums "2" and "3" is characterized by the loss-angle tangents γ_2 and γ_3. The depth z is counting from a surface, and the axis positive direction is down.

For investigation the frequency characteristics of normal waves the dispersion equation, determining the poles positions, can be conveniently written in the form:

$$1 + V \exp(2ib_1 h) = 0, \tag{1}$$

where b_1 is the vertical wave number in water layer, V is the layered bottom reflection coefficient.

The criteria, based on which the mode is classified as the "eigen" one for a waveguide with absorbing bottom, are the following: there is a pole, determined from (1), and the imaginary part of the vertical wave number in the half-space is negative [6].

3. FREQUENCY CHARACTERISTICS OF NORMAL WAVES

For numerical solution equation (1) was transformed to the form

$$-2hb_{1l} + (2l - 1)\pi - i\ln(V) = 0, \tag{2}$$

where $l = 1, 2, 3...$ is the mode number. The reflection coefficient V and the bottom input impedance Z_{in} were calculated with formulas [6, 14]:

$$V = \frac{Z_{in} - Z_1}{Z_{in} + Z_1}, \quad Z_{in} = \frac{Z_3 - iZ_2 \operatorname{tg}(b_2 d)}{Z_2 - iZ_3 \operatorname{tg}(b_2 d)} Z_2, \tag{3}$$

where b_2 is the vertical wave number in the intermediate layer "2", $Z_{1,2,3} = \omega\rho_{1,2,3}/b_{1,2,3}$ are the impedances of the layers "1", "2", and the half-space "3". The vertical wave numbers in the intermediate layer and the half-space in (3) were expressed in terms of $b_1 = b_{1l}$ using relations:

$$b_2 = b_{2l} = \sqrt{k_2^2 - \xi_l^2}, \quad b_3 = b_{3l} = \sqrt{k_3^2 - \xi_l^2}, \quad \xi_l = -\sqrt{k_1^2 - b_{1l}^2}, \tag{4}$$

where ξ_l is the horizontal wave number. The wave numbers in water and the intermediate layers and the half-space were given in the form: $k_1 = \omega/c_1$, $k_2 = \omega/c_2 - i\gamma_2$, $k_3 = \omega/c_3 - i\gamma_3$.

Equation (2) was solving by the intercept method [15]. Initial estimates of the roots were $0{,}5l\pi/h$ and $l\pi/h$.

In Fig. 1 the second quadrant of a complex plane of horizontally-wave numbers and the poles, which correspond to the eigenmodes on the frequency $f = 500$ Hz, are shown for a waveguide with parameters: $h = 20$ m, $d = 25$ m, $c_2/c_1 = 1{,}02$, $c_3/c_1 = 1{,}28$, $\rho_2/\rho_1 = 1{,}4$, $\rho_3/\rho_1 = 1{,}9$, $\gamma_2 = 0{,}001$, $\gamma_3 = 0{,}01$ (circles), $\gamma_2 = 0{,}01$, $\gamma_3 = 0{,}02$ (dots). The Pekeris sections, going from the branchpoints

of the second and the third radicals in (4), are marked by the vertical dotted lines. At smaller damping (circles) there are 13 eigenmodes, and 5 of them are the dissipative ones; and at grater damping (dots) there are 16 eigenmodes, and 8 of them are the dissipative ones. As seen from Fig. 1, the poles are not grouped between the Pekeris sections only, and they are placed along the hyperbolic line, which is similar to the Yuing-Zhardetski-Press section [5, 6, 16].

The frequency dependencies of real and imaginary parts of the vertical wave numbers in the half-space and water layer for a waveguide with $\gamma_2 = 0{,}01$ and $\gamma_3 = 0{,}03$ (other parameters are the same) are presented in Fig. 2.

The horizontal axis corresponds to the parametric frequency $k_1 h\nu/\pi$, and $\nu = \sqrt{1-(c_1/c_3)^2}$. As seen from Fig. 2a $\mathrm{Im}(b_{3l})$ changes approaching to the critical frequency, where $\mathrm{Im}(b_{3l}) = 0$.

Expression for the field in the half-space has the form of [7]: $p_{3l} = p_{2l}(h+d)\exp(-ib_{3l}(z-h-d))$. Separating the real and the imaginary parts of b_{3l}, we can write p_{3l} in a different way:

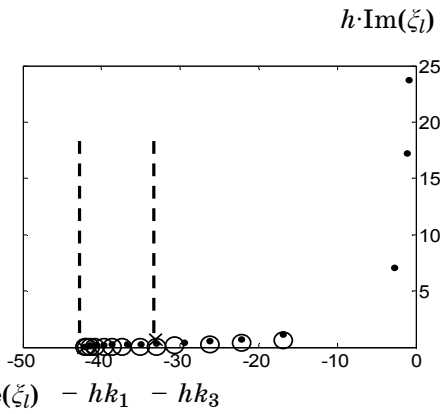

Fig. 1 *– Poles disposition on the horizontally-wave-number plane for two loss angle values*

$$p_{3l}(z) = p_{2l}(h+d)e^{\mathrm{Im}(b_{3l})(z-h-d)}e^{-i\,\mathrm{Re}(b_{3l})\cdot(z-h-d)} = \mid p_{3l} \mid e^{-i\arg(p_{3l})}\,.$$

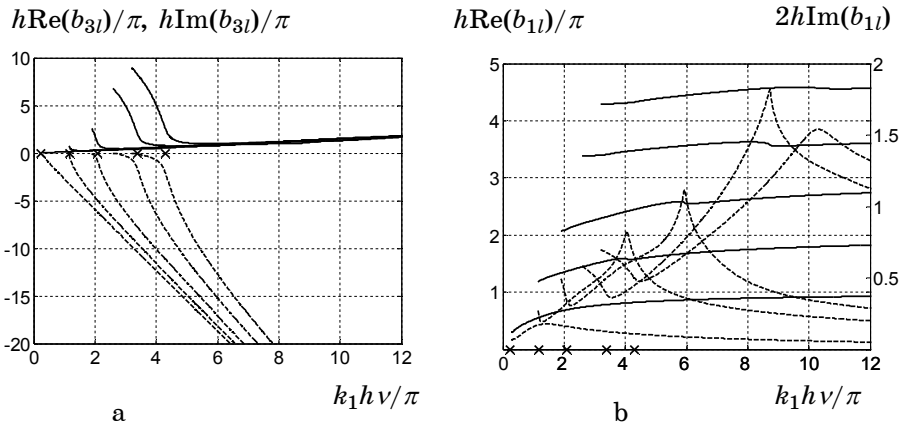

Fig. 2 *– Frequency characteristics of the real and the imaginary parts of the vertical wave numbers: in the half-space (a), in water layer (b). × is the critical frequency for a waveguide without absorption, —— is the Re(b), and - - - - is the Im(b)*

It is possible to see, that $\mathrm{Im}(b_{3l})$ makes sense of the "vertical" damping coefficient, and $\mathrm{Re}(b_{3l})$ makes sense of the vertical spatial frequency of a normal wave. Contrariwise, $\arg(p_{3l}) = \mathrm{Re}(b_{3l})(z - h - d)$ is the initial phase of instantaneous field of the acoustic pressure, which not only depends on the frequency, but is unfixed with the depth as well, that means the energy leakage and dissipation in the half-space [17].

Diagrams of the real and the imaginary parts of the wave numbers in water layer are presented in Fig. 2b. The value of $h\mathrm{Re}(b_{1l})$ on the critical frequency is less than $(2l - 1)\pi/2$, which is typical for the Pekeris model [18], due to the intermediate layer presence.

As seen from the dispersion equation (1), presented in the form of

$$V_l = e^{-2h\,\mathrm{Im}(b_{1l})} e^{i(\pi(2l-1)-2h\,\mathrm{Re}(b_{1l}))} = \mid V_l \mid e^{i\arg(V_l)},$$

$\mathrm{Im}(b_{1l})$ defines the modulus of the reflection coefficient, and $\mathrm{Re}(b_{1l})$ defines its phase. $\mathrm{Im}(b_{1l})$ increase leads to the decrease of $|V|$ and the growth of the sound energy leakage into bottom. On the high frequencies, where $\mathrm{Im}(b_{1l}) \to 0$, $|V| \to 1$ and $\arg(V) \to -\pi$.

Frequency dependences of the modulus and the phase of the reflection coefficient V versus the parameter $fh/c_1 = h/\lambda$ (f is the frequency, λ is the wavelength in water layer) are presented in Fig. 3. The modulus of the reflection coefficient on the certain frequency has a minimum, corresponding to the maximal acoustic "transparency" of the intermediate layer. This minimum occurs due to the wave interference, reflected from the interface water/intermediate layer and intermediate layer/half-space. Below the critical frequency for a waveguide without absorption (it is marked by the crosses on the horizontal axis) $|V|$ monotonically decreases.

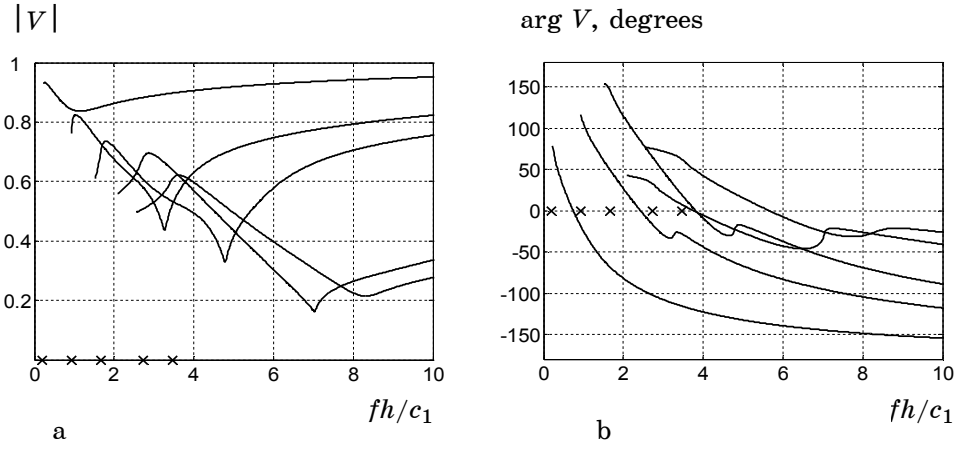

Fig. 3 *– Frequency dependences of the modulus and the phase of the reflection coefficient. The 1st-5th modes*

In Fig. 4 we present the frequency dependences of the bottom input impedance for the 1-st and the 2-nd modes and the vertical profiles of the second mode, calculated with formulas [19]:

in water layer: $p_{1l} = \sin(b_{1l}z)$,

in the intermediate layer: $p_{2l} = (A\sin(b_{2l}z) + B\cos(b_{2l}z))\rho_2/\rho_1$,

where $$A = \frac{b_{1l}}{b_{2l}}\cos(b_{2l}h)\cos(b_{1l}h) + \frac{\rho_1}{\rho_2}\sin(b_{2l}h)\sin(b_{1l}h)\,,$$

$$B = -\frac{b_{1l}}{b_{2l}}\sin(b_{2l}h)\cos(b_{1l}h) + \frac{\rho_1}{\rho_2}\cos(b_{2l}h)\sin(b_{1l}h)\,.$$

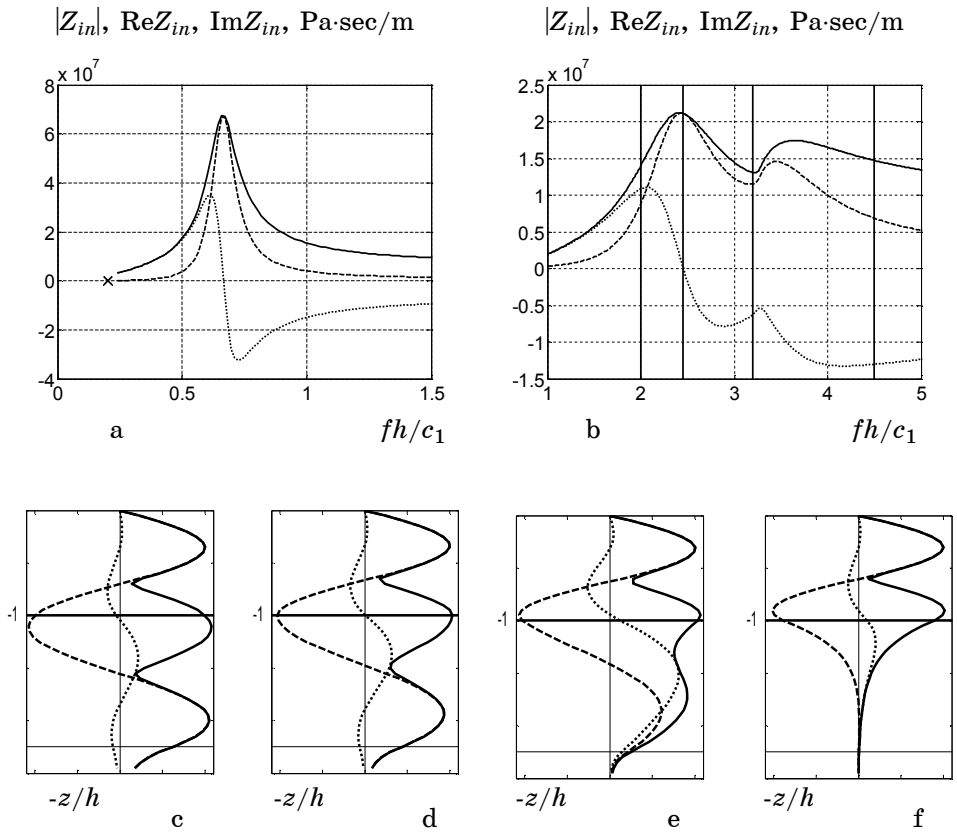

Fig. 4 *– Frequency dependences of the bottom input impedance for the first (a) and the second (b) modes and the vertical profiles p(z) of the second mode (c-f). Lines: — is the modulus, ----- is the active (real) component, ····· is the reactive (imaginary) component*

Frequency characteristics of the bottom input impedance for the 1-st mode have the "single-humped" form, for the 2-nd and higher modes they have the "double-humped" form as a result of the above-mentioned interference phenomena. Increase of the ratio c_2/c_1 leads to the peaks sharpening. With growth of the intermediate layer depth the extremum on the frequency

dependence of the bottom impedance for the 1-st mode displaces to the region of higher frequencies what is explained by the maximum moving off on the mode profile far from the interface water/intermediate layer. For higher modes the changes of the intermediate layer depth influence on the "saddle" part only, not acting to the left and the right slopes of the frequency characteristics (see Fig. 4b).

Consider the vertical profiles of the 2-nd mode (trapped) on four frequencies (see Fig. 4c-f), marked in Fig. 4b by the vertical firm lines. Interfaces of the water and the intermediate layers are denoted in Fig. 4c-f by the horizontal thick and thin lines, respectively. On the upper frequency ($h/\lambda = 4{,}5$) the second field maximum of the modulus $|p_2(z)|$ is in the water layer, and in the intermediate layer it aperiodically decreases (see Fig. 4f). With frequency decrease ($h/\lambda = 3{,}2$, see Fig. 4e) the second field maximum approaches to a bottom, and in the intermediate layer the field gradually becomes oscillatory. In Fig. 4d ($h/\lambda = 2{,}45$) the second field maximum coincides with a bottom, $\mathrm{Im}(p_2(z)) = \mathrm{Im}(Z_{in}) = 0$, $|Z_{in}|$ has a maximum, and the phase of reflection coefficient of the second mode (see Fig. 3b) equals to zero. On the lower frequency ($h/\lambda = 2$), Fig. 4c, the second field maximum moves into the intermediate layer, and the reactive component of the bottom input impedance changes a sign. Here $\arg V > 0$.

Frequency dependences of the modal absorption coefficient $\alpha_l = 8{,}68\mathrm{Im}(\xi_l)$ are presented in Fig. 5. If the intermediate layer depth $d < h$ it substantially influences not only on the modes with a number of $l > 1$ (see Fig. 5a). Under increase of the layer depth more than h the absorption maximums become less sharp and move down along the frequency axis. If there is the low-velocity layer (see Fig. 5b) the conditions for sound propagation are lowest, and the absorption coefficient of the 1-st mode increases almost by an order.

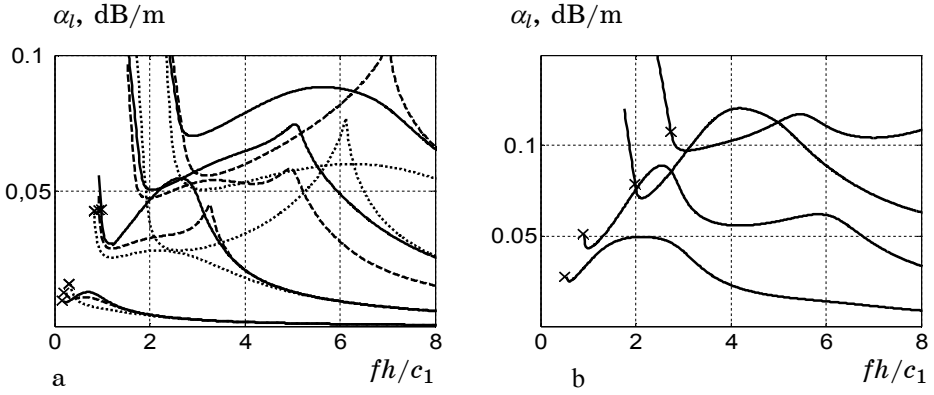

Fig. 5 *– Frequency dependencies of the modal absorption coefficient of the 1st-4th modes: for different intermediate layer depth, $c_2 \geq c_1$, (·····) d = 10 m, (----) d = 25 m, (—) d = 40 m (a); for the case $c_2 \leq c_1$, d = 10 m (b)*

The criterion for mode detection in a channel is the following [6]: the absorption value for the line length, which is equal to the tenfold channel depth, should not exceed 10 dB, what is 0,05 dB/m for a channel with h = 20 m. Taking into account the foregoing criterion one can conclude that

the field in layered waveguides on low frequencies ($h/\lambda < 8$) will be formed by the 1-st, 2-nd, and partly by the 3-d trapped modes. Surely, the mentioned estimation is applicable for the very shallow sea only. Frequency dependencies of the phase $\upsilon_l = \omega/\mathrm{Re}(\xi_l)$ and the group $u_l = \delta\omega/\delta(\mathrm{Re}(\xi_l))$ modes velocities are presented in Fig. 6.

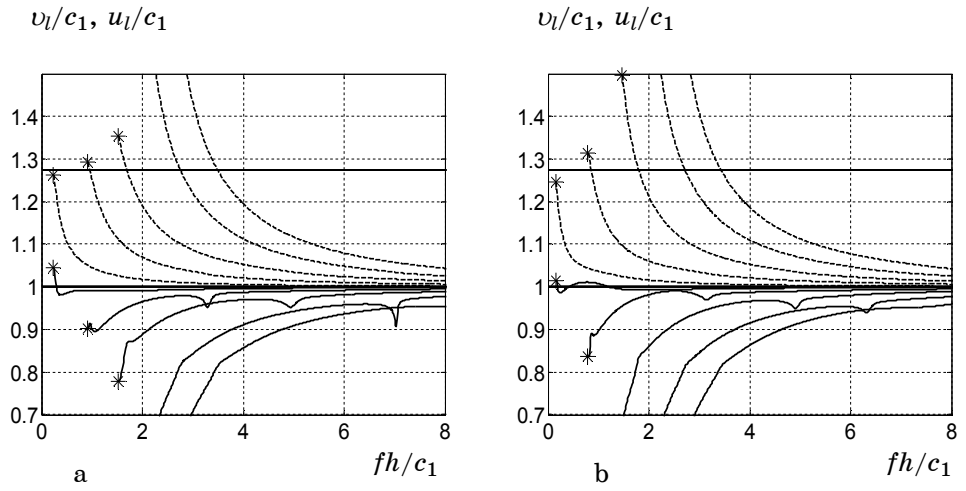

Fig. 6 *– Frequency dependencies of the phase (dotted line) and the group (solid line) velocities; d = 25 m (a); d = 50 m (b)*

The ratio c_3/c_1 is marked by the solid horizontal line. Frequency characteristic of the group velocity of the 1-st mode is almost of the classical type [7], with two maximums. The group velocity u_1 on the critical frequency (it is marked by the asterisk) in Fig. 6 does not reach the sound speed c_3 in the half-space only because of the calculation discreteness of wave numbers and derivative determination. The phase velocities of higher modes on the frequency, lower than the critical one, for a waveguide without absorption (it is easily determined as intersection of the phase velocity curve and the horizontal c_3/c_1) increase more than c_3, but the group velocities sharply decrease. This is the display of increasing absorption under approach to the critical frequency. The second maximum $u_l(f)$ is formed under dispersion laws separation in two subwaveguides, and the group velocities of different modes on the certain frequency can be found to be very close to each other or even equal (see Fig. 6b, the 1-st and the 2-nd modes). The intermediate layer is displayed also in the following: at the certain sound speed c_2 on the certain frequency there is deep minimum of the group velocity. The modulus of reflection coefficient $|V_l|$ (see Fig. 3a) and the modal absorption coefficients α_l (see Fig. 5a) on the same frequencies have the corresponding extremums. Here a power leakage through the intermediate layer to the half-space is maximal.

Frequency characteristics of the group velocity of the 1-st mode at different depths and various sound speeds in the intermediate layer are shown in Fig. 7.

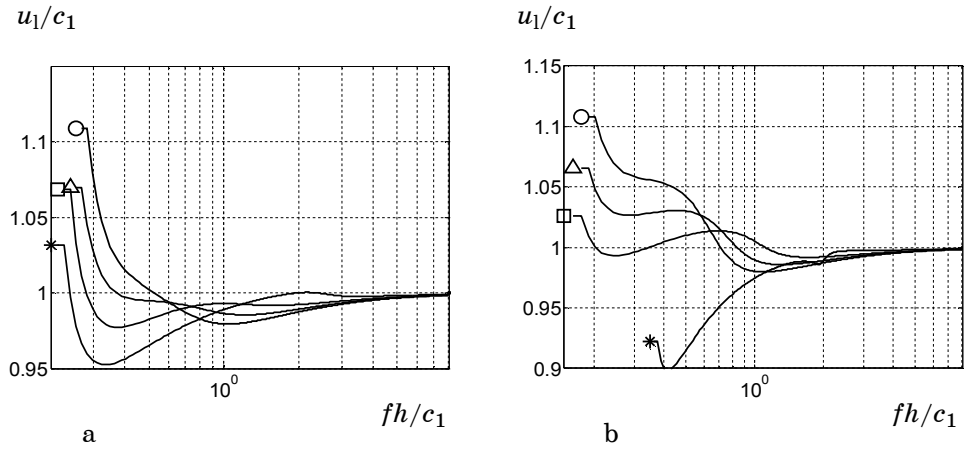

Fig. 7 *– Frequency dependencies of the group velocity of the first mode at differen sound speeds c_2 in the intermediate layer: d = 25 m (a); d = 50 m (b). c_2, m/sec* 1500 *(*);* 1550 *(□);* 1600 *(Δ);* 1650 *(O)*

The frequency axis scale is logarithmical. The closer ratio c_2/c_1 to the unity, the sharper the first minimum and the weaker expressed the second maximum of group velocity (convergence with the Pekeris model). With essential difference between sound speeds in water and in a layer ($c_2/c_1 \geq 1{,}1$, $d/h = 1{,}25$) the dispersion laws do not practically separate as well, and maximums of u_1 almost interflow – the trilaminar waveguide model approaches to the Pekeris model again. For a "thick" intermediate layer the dispersion laws separation and coalescence under increase of c_2/c_1 from 1 to c_3/c_1 are more clearly defined, the group velocity between the 1-st and the 2-nd its maximums exceeds c_1. In the frequency range, where $c_1 < u_1 < c_2$, the glancing angle of equivalent ray is closed to the critical one, and the sound wave propagates in the inter-mediate layer, reflecting from its boundaries.

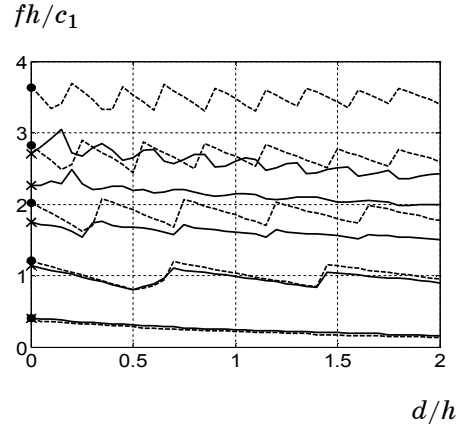

Fig. 8 *– Dependences of the critical frequency versus the intermediate layer depth for the 1st-5th modes. The dotted lines correspond to a waveguide without absorption, the solid lines – to a waveguide with absorption*

Dependences of the critical mode frequency, the modulus, and the phase of reflecting coefficient versus the intermediate layer depth and the vertical profiles of the 2-nd mode are presented in Fig. 8 and Fig. 9. In Fig. 8 the critical frequencies of nonabsorbing and absorbing waveguides are marked by the dots and the crosses, respectively, on the vertical axis (when $d \to 0$ there is the transition to the Pekeris model).

Dependences of the critical frequency and the modulus of the reflecting coefficient versus the layer depth are monotone for the 1-st mode only, and for higher modes they are complexly oscillatory. The oscillations excursion for absorbing waveguide decreases while the layer depth increases, and for the waveguide without absorption it does not practically change. The phase of the reflecting coefficient under the growth of the inter-mediate layer depth increases from 0 ($d = 0$) to π ($d/h = 0{,}6$), and here minimum of the acoustic field modulus on a mode profile gradually moves from water layer and approaches to a bottom. When $d/h = 0{,}6$ the value of reflecting coefficient is maximal, and the exponential tail on the mode profile in the half-space attenuates with the depth most rapidly. Under the layer depth growth up to $d/h = 0{,}7$ the value of $|V_2|$ harply decreases, the phase tends to 0 again, and the field minimum retraces to a water layer stratum. With further increase of the intermediate layer depth the phase of reflecting coefficient growths again tending to π, and the field minimum approaches to a bottom again. The traveling-wave factor, calculated as the ratio of amplitudes in the node and the antinode, for the 1-st, the 3-d, and the 4-th profiles (see Fig. 9c, e, f) is equal to 0,12, and for the 2-nd profile (see Fig. 9d) it is equal to 0,08.

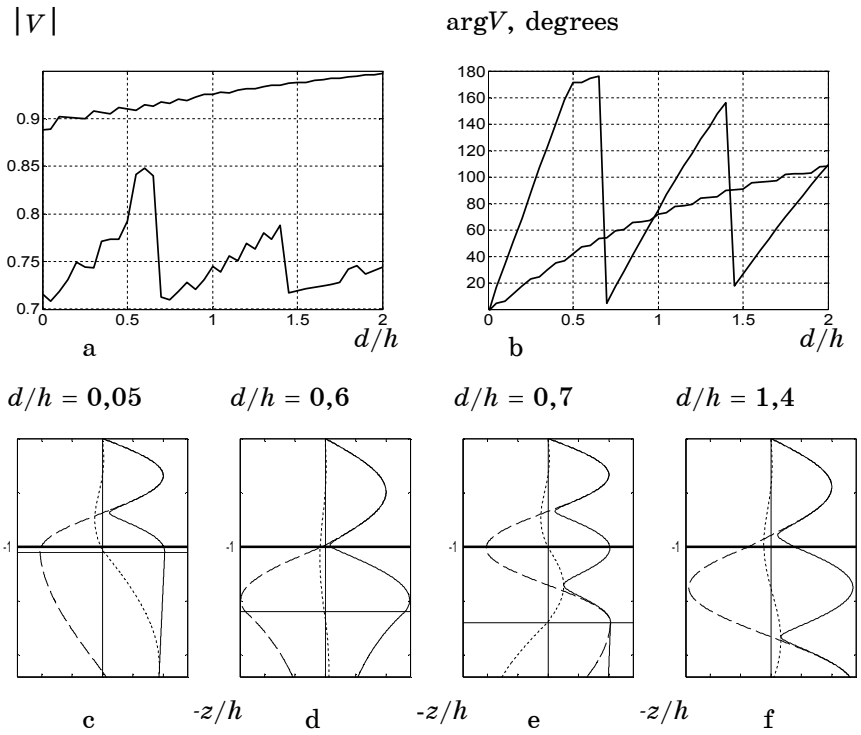

Fig. 9 *– Dependences of the modulus and the phase of reflecting coefficient on the critical frequency of the 1-st and the 2-nd modes (a, b) and changes of the 2-nd mode profile (c-f) versus the intermediate layer depth: (——) |p(z)|; (-----) Re p(z); (·····) Im p(z)*

4. CONCLUSIONS

One can expect the display of dissipative modes, probably, in water areas of the very shallow sea with homogeneous (to the depth ~ $2h$) bottom, formed by coarse-grained sand or shells, for which both the loss angle and the sound speed are maximal.

In water areas with layered bottom the determining influence on the acoustic field has a layer, adjacent with water one, under condition of its sufficient depth. The ground layers, lying below, influence weekly on the sound field, so it is possible to represent them as the half-space with equivalent parameters. Modes with numbers $l < 4$ make a dominating contribution into acoustic field on low frequencies ($h/\lambda < 10$).

The intermediate layer depth, within which it has the largest effect on the acoustic field in the very shallow sea, can be enclosed to the range of $0{,}25 < d/h < 2$. Outside this range the frequency dependencies of normal waves in a layered model approach to the similar ones for the Pekeris model. In layered waveguides the critical modes frequency with numbers $l > 1$ depends complexly on the loss angle and the layers depth.

Frequency characteristics of the phase and the group velocities for a waveguide with absorption essentially differ from the classical ones (for a waveguide without absorption). Frequency ranges with rised absorption correspond to the considerably lowered group velocity of the modes.

REFERENCES

1. N.S. Ageeva, V.D. Krupin, *Akust. zhurnal* **XXV** No3, 340 (1979).
2. N.S. Ageeva, V.D. Krupin, *Akust. zhurnal* **XXVI** No2, 161 (1980).
3. N.S. Ageeva, *Akustika okeana. Sovremennoe sostoyanie*, 107 (M.: Nauka: 1982).
4. B.A. Kasatkin, *Akustika okeana. Doklady 9-oy shkoly-seminara akademika L.M. Brehovskih, XII sessiya RAO*, 144 (M.: GEOS: 2002).
5. B.A. Kasatkin, N.V. Zlobina, *Akustika okeana. Doklady 11-oy shkoly-seminara akademika L.M. Brehovskih, XVII sessiya RAO*, 86 (M.: GEOS: 2006).
6. M.J. Buckingham, E.M. Giddens, *J. Acoust. Soc. Am.* **119** No1, 123 (2006).
7. L.M. Brehovskih, *Volny v sloistyh sredah* (M.: Nauka: 1973).
8. N.S. Ageeva, V.D. Krupin, *Akust. zhurnal* **XXVII** No5, 669 (1981).
9. B.G. Katsnel'son, V.G. Petnikov, *Akustika melkogo morya* (M.: Nauka: 1997).
10. O.N. Grudskaya, S.M. Grudskiy, E.A. Rivelis, *Akust. zhurnal* **XXXV** No6, 1054 (1989).2
11. S.J. Levinson, E.K. Westwood, R.A. Koch, S.K. Mitchell, C.V. Sheppard, *J. Acoust. Soc. Am.* **97** No3, 1576 (1995).
12. V.T. Grinchenko, I.V. Vovk, V.T. Matsypura, *Osnovy akustyky* (K.: Naukova dumka: 2007).
13. V.K. Bogushevich, L.N. Zamarenova and M.I. Skipa, *Physical Oceanography* **13** No5, 279 (2003).
14. L.M. Brehovskih, O.A. Godin, *Akustika neodnorodnyh sred: v 2 t. T.1: Osnovy teorii otrazheniya i rasprostraneniya zvuka* (M.: Nauka: 2007).
15. D. Matthewz, K. Fink, *Numerical methods using MATLAB, Fourth Edition* (New Jersey: Prentice-Hall Pub. Inc.: 2004).
16. Dj.De Santo, *Akustika okeana* (M.: Mir: 1982).
17. B.I. Goncharenko, L.N. Zaharov, V.E. Ivanov, *Akust. zhurnal* **XXV** No4, 507 (1979).
18. F.I. Kryazhev, N.A. Petrov, *Akust. zhurnal* **VI** No2, 229 (1960).
19. I. Tolstoy, K. Kley, *Akustika okeana. Teoriya i eksperiment v podvodnoy akustike* (M.: Mir: 1969).